Construction of Fractal Order and Phase Transition with Rydberg Atoms

Nayan E. Myerson-Jain, Stephen Yan[®], David Weld[®], and Cenke Xu[®] Department of Physics, University of California, Santa Barbara, California 93106, USA

(Received 3 September 2021; accepted 8 December 2021; published 5 January 2022)

We propose the construction of a many-body phase of matter with fractal structure using arrays of Rydberg atoms. The degenerate low energy excited states of this phase form a self-similar fractal structure. This phase is analogous to the so-called "type-II fracton topological states." The main challenge in realizing fractonlike models in standard condensed matter platforms is the creation of multispin interactions, since realistic systems are typically dominated by two-body interactions. In this work, we demonstrate that the van der Waals interaction and experimental tunability of Rydberg-based platforms enable the simulation of exotic phases of matter with fractal structures, and the study of a quantum phase transition involving a fractal ordered phase.

DOI: 10.1103/PhysRevLett.128.017601

In recent years, tremendous progress has been made in simulating quantum many-body systems with tunable arrays of Rydberg atoms [1–3]. In many such experiments, the ground state and a high-lying excited state of the atom constitute a qubit, the fundamental element of numerous exotic quantum many-body states [4,5]. Recently, the construction of unconventional many-body states like Z_2 quantum spin liquids has been explored [6–8], demonstrating the potential of the Rydberg-based platforms. The possibility to extend these platforms to realize quantum many-body systems beyond the currently well-understood theoretical paradigm such as those exhibiting Z_2 topological order [9–11] would be extremely exciting.

"Fracton" phases of matter provide a natural playground for exotic physics. These phases host excitations with restricted dynamics, and a ground-state degeneracy that scales with the system size [12–19]. Fracton related models are loosely classified by their qualitative features: "type-I" models have excitations whose dynamics are restricted to standard submanifolds, e.g., lines and planes in space, while excitations of the more exotic "type-II" models are created at the end of a fractal subset of the lattice [17]. While fracton and related phases are of great theoretical interest, much less progress has been made in realizing such models experimentally.

In this work, we propose an experimental realization of "fractal order," a two-dimensional analogue of a type-II fracton phase, as well as a quantum phase transition between the phase with fractal order and a trivial phase. The fractal order spontaneously breaks a fractal subsystem symmetry, and its low energy excitations form a Sierpinski triangle on the lattice, which is a fractal shape with Hausdorff dimension $d_H = \ln 3/\ln 2$, and only costs energy at the corners of the Sierpinski triangle. We stress that the fractal order we consider is defined as spontaneous

breaking of a fractal subsystem symmetry; this phase does not have topological order.

The Sierpinski triangle model [15,20] is the paradigmatic model with fractal order. It is a classical statistical mechanical model for an Ising system on a triangular lattice whose Hamiltonian is a sum over all three-body interactions on downward facing unit triangles ∇ (Fig. 1):

$$H_{\rm ST} = \sum_{\nabla} -K\sigma_1^z \sigma_2^z \sigma_3^z,\tag{1}$$

where the $\sigma^z = \pm 1$ are Ising degrees of freedom at the vertices of each downward triangle. The low energy excited states of this model have a fractal structure: starting with the obvious ground state with uniform $\sigma^z_j = +1$, low-lying excited states are created by flipping spins in the shape of a

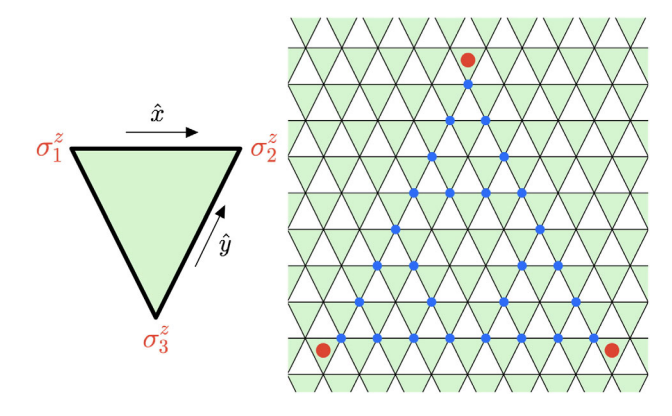


FIG. 1. Left: three-body spin interaction on each downward triangle in Eq. (1). Right: one of the low energy excitations of Eq. (1); starting with the obvious ground state with $\sigma^z = +1$, the spins are flipped to $\sigma^z = -1$ on a $\ell = 3$ Sierpinski triangle (blue), this configuration only costs energy on the unit triangles at the three corners (red).

Sierpinski triangle, which does not cost energy anywhere except at the three corners. The corners of the Sierpinski triangle can be viewed as point particles, which cannot move along the lattice without creating more excitations that cost higher energy. Hence the mobility of these particles is highly restricted; it is in this sense that they are fractons.

A quantum version of the Sierpinski triangle model was discussed in Ref. [21,22]. The quantum Sierpinski triangle model has an extra transverse field

$$H_{qST} = \sum_{\nabla} -K\sigma_1^z \sigma_2^z \sigma_3^z - \sum_j h \sigma_j^x$$
 (2)

and has two highly desirable features: (1) It is "self-dual," meaning that under a duality transformation the K and hterms will exchange. This self-duality is analogous to the Kramers-Wannier duality of the 1D quantum Ising model [23,24], and the self-duality of the quantum plaquette model [25]. The self-duality implies that, if there were a quantum phase transition reached by tuning h/K in Eq. (2), it must happen at h = K. (2) Numerical simulation of the quantum Sierpinski triangle model suggests that the system may have a second order quantum phase transition (QPT) at the self-dual point h = K [22] (though earlier numerics suggested a first order transition [21]); at the QPT, the energy density has a fractal dimension $d_H = \ln 3 / \ln 2$ rather than scaling dimension 2 as in ordinary QPT in 2D [22]. This transition is associated with the spontaneous breaking of a "fractal symmetry"; the phase with h < K is identified as a fractal order, while the phase with h > K is a disordered phase of the fractal symmetry [see the Supplemental Material (SM) [26] for more discussion].

The nature of the QPT at h = K in Eq. (2) is far from being understood, and the ordinary Landau-Ginzburg paradigm no longer applies. Numerics suggest that this transition is likely continuous, but many questions remain open. For example: Is the continuous QPT stable against perturbations? For ordinary transitions, this question is answered through the renormalization group (RG) method [27–29], by evaluating the relevance or irrelevance of certain perturbations. But for the QPT under discussion, no reliable RG procedure has been established. Hence, key aspects of the QPT must be explored experimentally. A tunable experimental realization of the classical and quantum Sierpinski triangle model would be extremely useful in understanding transitions involving fractal geometry.

The goal of this work is to describe a construction of both the classical and quantum Sierpinski triangle models from arrays of Rydberg atoms. We begin with a single atom whose ground state $|g\rangle$ is coupled to an excited Rydberg state $|r\rangle$ via a laser detuned from resonance. The two states coupled by the laser are the atom-field product states labeled $|g, N_{\gamma} + 1\rangle$ and $|r, N_{\gamma}\rangle$, where N_{γ} is the photon number of the laser so that $|g, N_{\gamma} + 1\rangle$ has one extra

photon compared to $|r,N_{\gamma}\rangle$. In the effective two-state problem, the Rabi frequency enters as a term coupling these two states. The simplest manifestation of the Rabi oscillations is as a term in the Hamiltonian $\Omega\sigma^x$ where $\sigma^x = |g,N_{\gamma}+1\rangle\langle r,N_{\gamma}| + |r,N_{\gamma}\rangle\langle g,N_{\gamma}+1|$.

If we blue-detune the laser from resonance, the energy gained by the atom being in the excited state $|r,N_{\gamma}\rangle$ relative to being in $|g,N_{\gamma}+1\rangle$ is $-\delta$, where δ is the detuning of the laser. This detuning then contributes a diagonal term to the effective Hamiltonian $-\delta\hat{n}$ where \hat{n} is 0 or 1 if the atom is in the state $|g,N_{\gamma}+1\rangle$ or $|r,N_{\gamma}\rangle$, respectively. This allows us to write down an effective two-state Hamiltonian in the basis of atom-field product states for the single atom

$$H_{1 \text{ atom}} = \Omega \sigma^{x} - \delta \hat{n}. \tag{3}$$

Two atoms in s-orbital Rydberg states interact through a force that can be modeled by a van der Waals (vdW) potential $V(r) = C/r^6$ when the separation r is large, where C is a constant that scales strongly with the principal quantum numbers. For two identical Rydberg atoms with principal quantum number n (not to be confused with the number operator \hat{n}), the coefficient C of the vdW interaction roughly scales as $\sim n^{11}$. In the remaining of the Letter we will use the more detailed evaluation of the vdW interaction given in Ref. [30]. As such, the total effective many-body Hamiltonian that describes a lattice of these atoms is

$$H = \sum_{i} \Omega_{i} \sigma_{i}^{x} + H_{0}, \qquad H_{0} = -\sum_{i} \delta_{i} \hat{n}_{i} + \sum_{ij} V_{ij} \hat{n}_{i} \hat{n}_{j},$$

$$\tag{4}$$

where $V_{ij} = C_{ij}/|i-j|^6$ and i, j label the lattice sites.

We start with the small Rabi frequency (relative to the detuning) limit of this model so that we may first ignore the σ^x terms and focus on the classical part of the Hamiltonian H_0 . To realize the classical Sierpinski triangle model of Eq. (1), we must select the parameters in H_0 which yield low energy states that can be mapped to those of the Sierpinski triangle model. We consider the honeycomb lattice with two sublattices A and B, trapping an "auxiliary" atom at each site in A and a "target" atom at each site in B. An equivalent picture is that we take the triangular lattice and decorate each vertex with a target atom and the center of each downward facing triangle with an auxiliary atom (Fig. 2). We aim to reproduce the states of Eq. (1) only on the \mathcal{B} sublattice with target atoms. The auxiliary atoms enlarge the Hilbert space and hence the states of model Eq. (1) with multispin interactions can be reproduced through two-body interactions only in the low energy subspace of the atomic system.

We assign different principal quantum numbers n_A and n_B for the Rydberg states of the auxiliary atoms on sublattice A and target atoms on sublattice B. With a

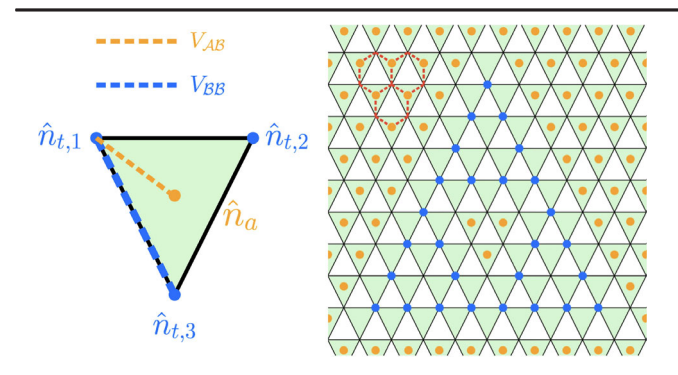


FIG. 2. We propose trapping atoms on both the vertices and the center of each downward triangle of the triangular lattice, which together form a honeycomb lattice. Vertices (centers) contain "target" ("auxiliary") atoms. A Sierpinski triangle excited state is shown where $\hat{n}_t = 1$ (blue) and $\hat{n}_a = 0$ (orange). The Hamiltonian Eq. (5) reduces to V_{AB} between auxiliary and neighboring target atoms, and interaction V_{BB} between neighboring target atoms.

proper choice of n_A , n_B , and the detuning, the Hamiltonian H_0 can be organized as $H_0 = \sum_{a \in A} H_{0,a}$:

$$H_{0,a} = V(2\hat{n}_a + \hat{n}_{t,1} + \hat{n}_{t,2} + \hat{n}_{t,3} - 2)^2 + \sum_{i=1}^3 v \hat{n}_a \hat{n}_{t,i}$$

$$\sim V\left(\sum_{i=1}^3 4\hat{n}_a \hat{n}_{t,i} + \sum_{i< j} 2\hat{n}_{t,i} \hat{n}_{t,j} - 4\hat{n}_a - \sum_{i=1}^3 3\hat{n}_{t,i}\right)$$

$$+ \sum_{i=1}^3 v \hat{n}_a \hat{n}_{t,i} \cdots. \tag{5}$$

The sum $H_0 = \sum_{a \in \mathcal{A}} H_{0,a}$ is over all sublattice sites \mathcal{A} , and each term in the sum involves an auxiliary atom $(\hat{n}_a = 0, 1)$ and its three neighboring target atoms $(\hat{n}_{t,i} = 0, 1)$ which form a downward triangle on the honeycomb lattice. The second line of Eq. (5) uses the fact that $\hat{n}_a^2 = \hat{n}_a$, $\hat{n}_t^2 = \hat{n}_t$ for $\hat{n} = 0, 1$. H_0 contains a two-body repulsive interaction $V_{\mathcal{A}\mathcal{B}} = 4V + v$ between the auxiliary atom and neighboring target atoms, as well as a repulsive interaction $V_{\mathcal{B}\mathcal{B}} = 2V$ between two nearest neighbor target atoms (Fig. 2).

When v > 0, there are two classes of configurations of $(\hat{n}_{t,i}; \hat{n}_a)$ on each downward triangle, both of which are the ground states of H_0 :

$$\begin{array}{ll} (1) \,\, \hat{n}_a = 1, & \quad \hat{n}_{t,i} = 0; \\ \\ \text{or} \quad (2) \,\, \hat{n}_a = 0, & \quad \text{two of} \,\, \hat{n}_{t,i} = 1. \end{array} \eqno(6)$$

As a comparison, the ground states of the classical Sierpinski triangle model $H_{\rm ST}$ also have two types of ground states on each downwards triangle:

(1)
$$\sigma_1^z = \sigma_2^z = \sigma_3^z = +1;$$

or (2) two of $\sigma_i^z = -1.$ (7)

Now the ground states of H_0 can be one-to-one mapped to the ground states of the classical Sierpinski triangle model, as long as we identify $\sigma_i^z = 1 - 2\hat{n}_{t,i}$. In the SM we will show that, all the states of Eq. (1) (ground and excited states) can be mapped one to one to the low energy subspace of H_0 when v > 0.

The relation between V_{AB} and V_{BB} can be tuned by choosing the principal quantum numbers n_A and n_B properly. For example, for potassium atoms, if we choose $n_A = 76$ and $n_B = 113$, then using the techniques in Ref. [30] and the fact that the interatomic distances are related by $r_{BB} = \sqrt{3}r_{AB}$, we found that both interactions are repulsive and satisfy $V_{AB}/V_{BB} \sim 2.628$ ($v \sim 1.26V$). Note that our results apply more broadly than just to this specific choice of atom and principal quantum numbers.

In the real system, there are perturbations to Eq. (5). These include other terms induced by the vdW interaction, for example, the repulsion between Rydberg states on two neighboring auxiliary atoms, whose strength $V_{\mathcal{A}\mathcal{A}}$ compared with $V_{\mathcal{B}\mathcal{B}}$ is $V_{\mathcal{A}\mathcal{A}}/V_{\mathcal{B}\mathcal{B}} \sim 0.011$ using the example parameters we chose above. The repulsion $V'_{\mathcal{B}\mathcal{B}}$ between the target atoms on two second neighbor \mathcal{B} sites is also much weaker than $V_{\mathcal{B}\mathcal{B}}$ due to the rapid decay of the vdW interaction with distance. Another notable perturbation is the interaction $V'_{\mathcal{A}\mathcal{B}}$ between an auxiliary atom and its nextneighbor target atom. Compared with $V_{\mathcal{B}\mathcal{B}}$, the two perturbations $V'_{\mathcal{B}\mathcal{B}}$ and $V'_{\mathcal{A}\mathcal{B}}$ are

$$\frac{V'_{\mathcal{B}\mathcal{B}}}{V_{\mathcal{B}\mathcal{B}}} = \frac{1}{(\sqrt{3})^6} \sim 0.037, \qquad \frac{V'_{\mathcal{A}\mathcal{B}}}{V_{\mathcal{B}\mathcal{B}}} = \frac{1}{2^6} \frac{V_{\mathcal{A}\mathcal{B}}}{V_{\mathcal{B}\mathcal{B}}} \sim 0.041. \tag{8}$$

These perturbations shift the energy of the excited state of the Sierpinski triangle shape. Let us consider an excited state with flipped "spins" ($\hat{n}_t = 1$) on a Sierpinski triangle with side length $L = 2^{\ell}$. In the ideal model of Eq. (1), the energy of this excited state does not depend on L or ℓ : all the energy cost arises from the corners of the Sierpinski triangle and the excitation energy $E_{\rm ex} = E - E_g = 6K = 3V = 3/2 \times V_{BB}$. However, in the real system the leading order perturbations V'_{AB} , V_{AA} , and V'_{BB} cause the energy of a Sierpinski triangle to scale with its size. In particular, the energy of the excitation relative to the ground state with uniform $\hat{n}_a = 1$ and $\hat{n}_t = 0$ is estimated to be (see SM for details)

$$E_{\text{ex}}^{\text{Ry}} = (3/2 - 0.1 + 0.47 \times 3^{\ell - 3}) V_{BB} \tag{9}$$

for Sierpinski triangles of $\ell \geq 2$. Since the actual energy cost of a Sierpinski triangle increases with its size, the perturbations can no longer be ignored for large enough Sierpinski triangles. Finite-size fractal excitations, however, are still observable.

Next, we outline a procedure to enable experimental observation of a spontaneously generated fractal-shaped

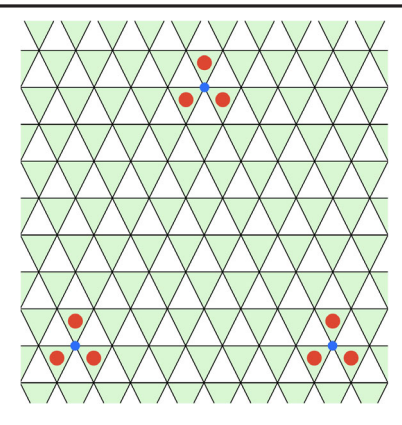


FIG. 3. With Hamiltonian Eq. (5), if three target atoms at the corners of a triangle with side length L=8 are excited from the ground state to the Rydberg state, it costs energy 3V+3v at each corner. If we apply an extra detuning $-\bar{\delta}_C\hat{n}_t$ on the three corners of the triangle, for sufficiently large $\bar{\delta}_C$ the ground state of the system is given by the fractal configuration in Fig. 1.

excitation. This can be done by adiabatically evolving a prepared ground state of Eq. (5) to the Sierpinski triangle excitation, which is the ground state of a new Hamiltonian achieved by slowly and carefully varying the detuning and Rabi frequency. Note that this procedure requires a level of local control beyond most current Rydberg experimental platforms, where focus has largely been on leveraging the Rydberg blockade mechanism to generate entanglement between adjacent sites [1,31,32]. Nevertheless, promising techniques which achieve elements of the desired single-site Rydberg control have already been demonstrated experimentally [33,34].

We start with the Hamiltonian of Eq. (5) with a small and finite Rabi frequency. To ensure a unique ground state (to enable an adiabatic evolution), we first deform Eq. (5) with a small extra detuning $\delta \hat{n}_t$ on all target atoms *outside of* a triangle with side $L = 2^{\ell}$. We then prepare an initial state with all target atoms $\hat{n}_t = 0$ and $\hat{n}_a = 1$, which is equivalent to $\sigma^z = 1$ uniformly in Eq. (1) and represents the unique ground state of the Hamiltonian prepared above. We slowly deform the Hamiltonian with time-dependent Rabi frequency $\Omega(t)$ and detuning $\delta_i(t)$ within the triangle, reaching the final Hamiltonian with extra detuning $-\bar{\delta}_C \hat{n}_t$ localized to three target atoms at the corners of the triangle (Fig. 3). Both Ω and δ are turned on inside the triangle during the evolution, which explicitly breaks all the symmetries of the finite system along the evolution path to avoid small gaps and ensure adiabaticity. With sufficiently large $\bar{\delta}_C$, the unique ground state of the final Hamiltonian contains a Sierpinski triangle configuration of the atoms inside the triangle, as shown in Figs. 1 and 2, despite the fact that in the final Hamiltonian the extra detuning $-\bar{\delta}_C \hat{n}_t$ is only applied locally at the corners rather than throughout the interior. Based on our estimate of energy in Eq. (9) which includes further neighbor repulsion arising from the vdW interaction, this phenomenon can hold up to Sierpinski triangles with $\ell=4$ (side length L=16, containing 81 atoms), as a single Sierpinski triangle configuration still has lower energy than fragmented configurations.

We have specified the initial and final Hamiltonian for the desired evolution; an adiabatic path of the detuning and Rabi frequency for observing Ising-like crystallization of Rydberg atoms has been demonstrated [31,32,35]. We can also arrive at the Sierpinski triangle ground state without adiabaticity. Leveraging either one of the aforementioned current or future techniques for single-site Rydberg control, we could realize the Sierpinski triangle configuration via local excitation to Rydberg states. Spectroscopic measurement of the energy of the Sierpinski configuration compared with that of fragmented configurations could then confirm that it represents a low-lying excited state.

This experimental platform also gives us the potential to probe QPTs by controlling the Rabi frequency. When the Rabi frequency Ω is increased uniformly on all target atoms, around $\Omega \sim V$ there is expected to be a QPT similar to the one recently studied numerically [21,22]. In the large Ω phase, one is not supposed to observe the fractal configuration in the proposed experiment above, i.e., the configuration of Fig. 3 will not evolve to the one in Figs. 1 and 2. As we pointed out before, the nature of this QPT is far from being understood. Hence the realization of the QPT in highly tunable experimental systems is crucial to understand these exotic transitions, as well as related theoretical paradigms developed in the future.

The fractal structure also manifests at the level of correlation functions. In both the classical and quantum Sierpinski triangle models, the three-point correlation function $C_3 = \langle \sigma_j^z \sigma_{j+L\hat{x}}^z \sigma_{j+L(\hat{x}-\hat{y})}^z \rangle$ is a characteristic quantity which plays the role of the correlation function of ordinary quantum many-body systems. The three-point correlation decays hyperexponentially with the Hausdorff dimension at finite temperature [15,20] and its scaling at the QPT h = K was computed in Ref. [22]. In the experimental realization of Eq. (5), the three-point correlation C_3 can be reconstructed by averaging over multiple single-site resolution snapshots of the configuration of the target atoms taken in separate experimental realizations. Similar techniques have been used previously in cold-atom experiments to reconstruct quantities such as the spin correlation functions in Fermi-Hubbard systems [36,37]. Experimental measurement of C_3 , whose scaling with distance diagnoses the fractal physics of the model, will be crucial in understanding the nature of this QPT.

Previous proposals for realizing fracton related states mostly focused on type-I fractons [38–41]; for example, efforts based on localized Majorana zero modes for both type-I and type-II states [42,43]. Compared with previous proposals, the platform of Rydberg atoms discussed in the current work is highly tunable with precision at the level of a single atom. Previously fractal structures were

constructed as a rigid background for electron states [44–46], while in our approach the fractal itself is the consequence of a quantum Hamiltonian, and the fractal structure can melt through a QPT with controllable parameters.

Another advantage of the platform of Rydberg atoms is fast manipulation of parameters in the Hamiltonian, which can either periodically drive the system, or cause a quantum quench [47-54]. Out of equilibrium dynamics of a cold atom system was also shown to probe topological features [55]. Many exotic features are expected in the quantum dynamics of fracton related models due to the restricted motion of fracton excitations [56–59]. By quickly tuning parameters such as the Rabi frequency in Eq. (4), one can compare the quantum dynamics of the fractal order simulated with Rydberg atoms with future analytical and numerical analysis. Even when Ω is tuned slowly, the fractal symmetry of the system may lead to unique critical dynamics near the QPT which are distinct from those in ordinary systems. Furthermore, our construction of Eq. (5) used to reproduce multispin interactions with only twobody interactions, can be extended to other fracton related models. One example of such extension (the Sierpinski tetrahedron model [60,61]) is given in the SM.

The authors thank Chao-Ming Jian and Hannes Bernien for helpful discussions. C. X. acknowledges NSF Grant No. DMR-1920434, and the Simons Investigator program. D. W. acknowledges support from the Army Research Office (MURI W911NF1710323). We acknowledge support via the UC Santa Barbara NSF Quantum Foundry funded via the Q-AMASE-i program under Grant DMR-1906325. This material is based in part upon work supported by the U.S. Department of Energy, Office of Science, National Quantum Information Science Research Centers, Quantum Science Center.

- [1] A. Browaeys and T. Lahaye, Nat. Phys. 16, 132 (2020).
- [2] C. Gross and I. Bloch, Science **357**, 995 (2017).
- [3] M. Saffman, T. G. Walker, and K. Mølmer, Rev. Mod. Phys. 82, 2313 (2010).
- [4] X.-G. Wen, Rev. Mod. Phys. 89, 041004 (2017).
- [5] S. Sachdev, Rep. Prog. Phys. 82, 014001 (2019).
- [6] R. Verresen, M. D. Lukin, and A. Vishwanath, Phys. Rev. X 11, 031005 (2021).
- [7] R. Samajdar, W. W. Ho, H. Pichler, M. D. Lukin, and S. Sachdev, Proc. Natl. Acad. Sci. U.S.A. 118, e2015785118 (2021), ISSN 0027-8424.
- [8] G. Semeghini, H. Levine, A. Keesling, S. Ebadi, T. T. Wang, D. Bluvstein, R. Verresen, H. Pichler, M. Kalinowski, R. Samajdar *et al.*, Science 374, 1242 (2021).
- [9] N. Read and S. Sachdev, Phys. Rev. Lett. 66, 1773 (1991).
- [10] X. G. Wen, Phys. Rev. B 44, 2664 (1991).
- [11] A. Kitaev, Ann. Phys. (Amsterdam) 303, 2 (2003), ISSN 0003-4916.
- [12] J. Haah, Phys. Rev. A 83, 042330 (2011).

- [13] C. Chamon, Phys. Rev. Lett. 94, 040402 (2005).
- [14] S. Bravyi, B. Leemhuis, and B. M. Terhal, Ann. Phys. (Amsterdam) 326, 839 (2011), ISSN 0003-4916.
- [15] B. Yoshida, Phys. Rev. B 88, 125122 (2013).
- [16] S. Vijay, J. Haah, and L. Fu, Phys. Rev. B 92, 235136 (2015).
- [17] S. Vijay, J. Haah, and L. Fu, Phys. Rev. B 94, 235157 (2016).
- [18] R. M. Nandkishore and M. Hermele, Annu. Rev. Condens. Matter Phys. 10, 295 (2019).
- [19] M. Pretko, X. Chen, and Y. You, Int. J. Mod. Phys. A **35**, 2030003 (2020).
- [20] M. E. J. Newman and C. Moore, Phys. Rev. E **60**, 5068 (1999).
- [21] L. M. Vasiloiu, T. H. E. Oakes, F. Carollo, and J. P. Garrahan, Phys. Rev. E 101, 042115 (2020).
- [22] Z. Zhou, X.-F. Zhang, F. Pollmann, and Y. You, arXiv: 2105.05851.
- [23] H. A. Kramers and G. H. Wannier, Phys. Rev. **60**, 252 (1941)
- [24] J. B. Kogut, Rev. Mod. Phys. 51, 659 (1979).
- [25] C. Xu and J.E. Moore, Phys. Rev. Lett. **93**, 047003 (2004).
- [26] See Supplemental Material at http://link.aps.org/supplemental/10.1103/PhysRevLett.128.017601 for (1) evaluation of the energy of a Sierpinski triangle excitation in real system; (2) mapping between the states of the Sierpinki triangle model to the Rydberg atom Hilbert space; (3) definition of the fractal symmetry; (4) discussion of the Sierpinski tetrahedron model.
- [27] K. G. Wilson, Phys. Rev. B 4, 3174 (1971).
- [28] K. G. Wilson and M. E. Fisher, Phys. Rev. Lett. 28, 240 (1972).
- [29] K. G. Wilson, Rev. Mod. Phys. 47, 773 (1975).
- [30] N. Šibalić, J. Pritchard, C. Adams, and K. Weatherill, Comput. Phys. Commun. 220, 319 (2017), ISSN 0010-4655
- [31] P. Scholl, M. Schuler, H. J. Williams, A. A. Eberharter, D. Barredo, K.-N. Schymik, V. Lienhard, L.-P. Henry, T. C. Lang, T. Lahaye *et al.*, Nature (London) **595**, 233 (2021).
- [32] S. Ebadi, T. T. Wang, H. Levine, A. Keesling, G. Semeghini, A. Omran, D. Bluvstein, R. Samajdar, H. Pichler, W. W. Ho *et al.*, Nature (London) **595**, 227 (2021).
- [33] H. Labuhn, S. Ravets, D. Barredo, L. Béguin, F. Nogrette, T. Lahaye, and A. Browaeys, Phys. Rev. A **90**, 023415 (2014).
- [34] X.-F. Shi, J. Phys. B 53, 054002 (2020).
- [35] P. Schauß, J. Zeiher, T. Fukuhara, S. Hild, M. Cheneau, T. Macrì, T. Pohl, I. Bloch, and C. Gross, Science 347, 1455 (2015), ISSN 0036-8075.
- [36] M. F. Parsons, A. Mazurenko, C. S. Chiu, G. Ji, D. Greif, and M. Greiner, Science 353, 1253 (2016), ISSN 0036-8075.
- [37] M. Endres, M. Cheneau, T. Fukuhara, C. Weitenberg, P. Schauß, C. Gross, L. Mazza, M. C. Bañuls, L. Pollet, I. Bloch *et al.*, Science **334**, 200 (2011), ISSN 0036-8075.
- [38] C. Xu and M. P. A. Fisher, Phys. Rev. B 75, 104428 (2007).
- [39] M. Pretko, Phys. Rev. B 100, 245103 (2019).
- [40] J. Sous and M. Pretko, Phys. Rev. B 102, 214437 (2020).
- [41] K. Giergiel, R. Lier, P. Surówka, and A. Kosior, arXiv: 2107.06786.

- [42] C. Xu and L. Fu, Phys. Rev. B 81, 134435 (2010).
- [43] Y. You and F. von Oppen, Phys. Rev. Research 1, 013011 (2019).
- [44] J. Shang, Y. Wang, M. Chen, J. Dai, X. Zhou, J. Kuttner, G. Hilt, X. Shao, J. M. Gottfried, and K. Wu, Nat. Chem. 7, 389 (2015), ISSN 1755-4349.
- [45] C. Li, X. Zhang, N. Li, Y. Wang, J. Yang, G. Gu, Y. Zhang, S. Hou, L. Peng, K. Wu *et al.*, J. Am. Chem. Soc. **139**, 13749 (2017), ISSN 0002-7863.
- [46] S. N. Kempkes, M. R. Slot, S. E. Freeney, S. J. M. Zevenhuizen, D. Vanmaekelbergh, I. Swart, and C. M. Smith, Nat. Phys. 15, 127 (2019), ISSN 1745-2481.
- [47] A. Polkovnikov, K. Sengupta, A. Silva, and M. Vengalattore, Rev. Mod. Phys. 83, 863 (2011),
- [48] K. Wintersperger, C. Braun, F. N. Ünal, A. Eckardt, M. D. Liberto, N. Goldman, I. Bloch, and M. Aidelsburger, Nat. Phys. 16, 1058 (2020), ISSN 1745-2481.
- [49] I.-D. Potirniche, A. C. Potter, M. Schleier-Smith, A. Vishwanath, and N. Y. Yao, Phys. Rev. Lett. 119, 123601 (2017).
- [50] K. Singh, C. J. Fujiwara, Z. A. Geiger, E. Q. Simmons, M. Lipatov, A. Cao, P. Dotti, S. V. Rajagopal, R. Senaratne, T. Shimasaki, M. Heyl, A. Eckardt, and D. M. Weld, Phys. Rev. X 9, 041021 (2019).
- [51] Z. Chen, T. Tang, J. Austin, Z. Shaw, L. Zhao, and Y. Liu, Phys. Rev. Lett. 123, 113002 (2019).

- [52] D. Bluvstein, A. Omran, H. Levine, A. Keesling, G. Semeghini, S. Ebadi, T. T. Wang, A. A. Michailidis, N. Maskara, W. W. Ho *et al.*, Science 371, 1355 (2021), ISSN 0036-8075.
- [53] A. Keesling, A. Omran, H. Levine, H. Bernien, H. Pichler, S. Choi, R. Samajdar, S. Schwartz, P. Silvi, S. Sachdev et al., Nature (London) 568, 207 (2019).
- [54] H. Bernien, S. Schwartz, A. Keesling, H. Levine, A. Omran, H. Pichler, S. Choi, A. S. Zibrov, M. Endres, M. Greiner et al., Nature (London) 551, 579 (2017).
- [55] M. Tarnowski, F. N. Ünal, N. Flaschner, B. S. Rem, A. Eckardt, K. Sengstock, and C. Weitenberg, Nat. Commun. 10, 1728 (2019), ISSN 2041-1723.
- [56] S. Pai and M. Pretko, Phys. Rev. Lett. 123, 136401 (2019).
- [57] A. Prem, J. Haah, and R. Nandkishore, Phys. Rev. B 95, 155133 (2017).
- [58] J. Feldmeier, P. Sala, G. De Tomasi, F. Pollmann, and M. Knap, Phys. Rev. Lett. 125, 245303 (2020).
- [59] I. H. Kim and J. Haah, Phys. Rev. Lett. 116, 027202 (2016).
- [60] J. P. Garrahan, J. Phys. Condens. Matter 14, 1571 (2002).
- [61] T. Devakul, Y. You, F. J. Burnell, and S. L. Sondhi, SciPost Phys. 6, 7 (2019).